Progress In Electromagnetics Research, Vol. 137, 19–34, 2013

EFFICIENT IMPLEMENTATION OF THE CAPON BEAMFORMING USING THE LEVENBERG-MARQUARDT SCHEME FOR TWO DIMENSIONAL AOA ESTIMATION

Sung-Woo Cho and Joon-Ho Lee*

Department of Information and Communication Engineering, Sejong University, Seoul, Korea

Abstract—In this paper, we adopt the Levenberg-Marquardt (LM) algorithm to implement the nonlinear multivariable optimization for azimuth/elevation angle-of-arrival (AOA) estimation based on the Capon beamforming algorithm. The formulation is based on the fact that the cost function of the Capon algorithm can be expressed in a least-squares form. The performance in terms of the root mean square error (RMSE) and the computational complexity is illustrated via numerical results.

1. INTRODUCTION

There have been many studies on array signal processing [1–38]. Angle-of-arrival (AOA) estimation [1–18] and beamforming [19–38] have been main research topics of the array signal processing. Note that array signal processing can also be applied to radar signal processing [39–43].

Capon beamforming algorithm [1], also called minimum variance beamforming algorithm, has been one of many algorithms on the determination of the AOA of incident signals using array antenna structure.

Basically, Capon beamformer is better than Bartlett beamformer in the viewpoint of resolution and interference rejection. The problem with Capon beamformer is that its performance is highly dependent on the preciseness of the knowledge of the AOA. Recently, there have been many studies to improve the robustness of the Capon beamformer to circumvent the problem induced by the differences between the true AOA and the assumed AOA [44–48].

Received 27 December 2012, Accepted 2 February 2013, Scheduled 7 February 2013
* Corresponding author: Joon-Ho Lee (joonhlee@sejong.ac.kr).

Our interest in this paper is to adopt the LM algorithm to implement nonlinear optimization for AOA estimation. We give an explicit numerical formulation for the improvement of azimuth/elevation AOA estimation for the uniform circular array (UCA) structure based on the Capon beamforming algorithm. The formulation for the Levenberg-Marquardt (LM) algorithm is based on the cost function derived from the Capon beamforming algorithm. A rigorous formulation of the LM-implementation of the Capon algorithm is presented.

For N incident signals, the cost function of the maximum likelihood (ML) algorithm [2, 3] is pN-dimensional, where p is the number of parameters to be estimated for each incident signal. For the estimation of azimuth angle, $p = 1$, the cost function is N-dimensional. For the simultaneous estimation of azimuth and elevation, $p = 2$, the cost function is $2N$-dimensional. Therefore, for large value of N, the optimization of pN-dimensional cost function by exhaustive grid search is not feasible. That is why Newton-type algorithms including the LM algorithm have been widely applied to the optimization of the cost function of the ML algorithm [2, 3].

Note that, in the Capon beamforming algorithm [1], the cost function is p-dimensional, which is independent of the actual number of the incident signals N. When we are only concerned with the estimation of the azimuth angle, the optimization of one-dimensional cost function using exhaustive grid search even with small search step is quite feasible. But, for simultaneous estimation of the azimuth and the elevation, the computational complexity of two-dimensional optimization by exhaustive grid search is much larger than that of one dimensional optimization by exhaustive grid search, which justifies why we apply the LM algorithm to the optimization of the two-dimensional cost function of the Capon beamforming algorithm.

There has been much study on applying the Newton-type method to the optimization of the cost function of the ML DOA algorithm [2, 3]. To the best of our knowledge, there has been no study on applying the LM algorithm to the optimization of the cost function of the Capon algorithm for simultaneous estimation of the azimuth angle and the elevation angle.

2. LM-BASED IMPLEMENTATION OF THE CAPON AOA ESTIMATION

Consider the case of a UCA with M antenna elements. N signals are incident on the array and we are to estimate the azimuth angle and the elevation angle of each incident signal. Note that, for simultaneous

estimation of the azimuth and the elevation, the uniform linear array (ULA) cannot be adopted since ULA-based algorithm cannot uniquely estimate the azimuth and the elevation due to the ambiguity pertinent to the ULA structure. Any array structure which is compatible with the simultaneous estimation of the azimuth and the elevation can be adopted.

In the Capon beamforming algorithm for AOA estimation, the array output power is computed as the arrival angle varies, and the local maxima in the output power distribution are considered to be the true directions of arrival.

Let θ and ϕ represent azimuth and elevation, respectively, which are the arrival angles of an interest [1]:

$$P(\theta,\phi) = \frac{1}{\mathbf{a}^{\mathrm{H}}(\theta,\phi)\hat{\mathbf{R}}^{-1}\mathbf{a}(\theta,\phi)} \equiv \frac{1}{F(\theta,\phi)} \tag{1}$$

where $F(\theta,\phi)$ is defined as

$$F(\theta,\phi) \equiv \mathbf{a}^{H}(\theta,\phi)\hat{\mathbf{R}}^{-1}\mathbf{a}(\theta,\phi), \tag{2}$$

and $\hat{\mathbf{R}}$ denotes an estimate of a covariance matrix of an array antenna.

The array vector can be written as

$$\mathbf{a}\,(\theta,\phi) = [\exp(j\psi_1)\ \exp(j\psi_2)\ \ldots\ \exp(j\psi_M)]^{\mathrm{T}} \tag{3}$$

where ψ_m for the UCA is defined as follows;

$$\psi_m\,(\theta,\phi) = 2\pi\frac{r}{\lambda}\cos\phi\left[\cos\left(\theta - \frac{2\pi(m-1)}{M}\right)\right] \quad m = 1,\ldots,M. \tag{4}$$

Let a vector valued function $\mathbf{f}(\theta,\phi)$ be in the form of

$$\mathbf{f}(\theta,\phi) = [\ f_1(\theta,\phi) \quad f_2(\theta,\phi) \quad \ldots \quad f_{2M}(\theta,\phi)\ ]^{\mathrm{T}}. \tag{5}$$

To apply the LM algorithm to the optimization of the Capon beamforming algorithm, we define $\mathbf{f}(\theta,\phi)$ so that $\|\mathbf{f}(\theta,\phi)\|_2^2$ corresponds to the cost function of $F(\theta,\phi)$ in (2). In that case, the Capon beamforming algorithm can be formulated as

$$\left[\hat{\theta},\hat{\phi}\right] = \arg\min_{\theta,\phi} F(\theta,\phi) = \arg\min_{\theta,\phi}\|\mathbf{f}(\theta,\phi)\|_2^2 = \arg\min_{\theta,\phi}\sum_{m=1}^{2M}|f_m(\theta,\phi)|^2. \tag{6}$$

Let $\mathbf{X}$ be defined as

$$\mathbf{X} = \begin{bmatrix} X_1(t_1) & \ldots & X_1(t_N) \\ \vdots & \ddots & \vdots \\ X_M(t_1) & \ldots & X_M(t_N) \end{bmatrix}, \tag{7}$$

where $X_m(t_n)$, $m = 1, \ldots, M$, $n = 1, \ldots, N$, refers to the incident signal received at the m-th antenna at $t = t_n$. Therefore, the m-th row of $\mathbf{X}$ corresponds to the received signals at the m-th antenna element at all time instants, and the n-th column of $\mathbf{X}$ corresponds to the received signal at all M antenna elements at the time instant $t = t_n$.

Based on the fact that the estimate of the covariance matrix is given by

$$\hat{\mathbf{R}} = \frac{1}{M}\mathbf{X}\mathbf{X}^{\mathrm{H}}, \tag{8}$$

we show how to express the cost function in (2) in least-squares form. Using (8) in (2), we have

$$\begin{aligned} F(\theta,\phi) &= \mathbf{a}^{\mathrm{H}}(\theta,\phi)\,\hat{\mathbf{R}}^{-1}\mathbf{a}(\theta,\phi) = M\mathbf{a}^{\mathrm{H}}(\theta,\phi)\left(\mathbf{X}\mathbf{X}^{\mathrm{H}}\right)^{-1}\mathbf{a}(\theta,\phi) \\ &= M\mathbf{a}^{\mathrm{H}}(\theta,\phi)\left(\mathbf{X}\mathbf{X}^{\mathrm{H}}\right)^{-1}\left(\mathbf{X}\mathbf{X}^{\mathrm{H}}\right)\left(\mathbf{X}\mathbf{X}^{\mathrm{H}}\right)^{-1}\mathbf{a}(\theta,\phi) \\ &= M\mathbf{a}^{\mathrm{H}}(\theta,\phi)\left(\mathbf{X}^{\mathrm{H}}\left(\mathbf{X}\mathbf{X}^{\mathrm{H}}\right)^{-1}\right)^{\mathrm{H}}\left(\mathbf{X}^{\mathrm{H}}\left(\mathbf{X}\mathbf{X}^{\mathrm{H}}\right)^{-1}\right)\mathbf{a}(\theta,\phi) \\ &= \left\|\sqrt{M}\mathbf{X}^{\mathrm{H}}\left(\mathbf{X}\mathbf{X}^{\mathrm{H}}\right)^{-1}\mathbf{a}(\theta,\phi)\right\|_2^2. \end{aligned} \tag{9}$$

In (9), note that $\sqrt{M}\mathbf{X}^{\mathrm{H}}(\mathbf{X}\mathbf{X}^{\mathrm{H}})^{-1}\mathbf{a}(\theta,\phi)$ is a column vector with M entries. Let the m-th entry of $\sqrt{M}\mathbf{X}^{\mathrm{H}}(\mathbf{X}\mathbf{X}^{\mathrm{H}})^{-1}\mathbf{a}(\theta,\phi)$ be denoted by $g_m(\theta,\phi)$:

$$\begin{aligned} g_m(\theta,\phi) &= \left(\sqrt{M}\mathbf{X}^{\mathrm{H}}\left(\mathbf{X}\mathbf{X}^{\mathrm{H}}\right)^{-1}\mathbf{a}(\theta,\phi)\right)_m \\ &= \sqrt{M}\sum_{n=1}^{N}\sum_{i=1}^{N}\Bigg\{\Bigg[\mathrm{Re}\left(\left(\mathbf{X}^{\mathrm{H}}\right)_{m,i}\left(\left(\mathbf{X}\mathbf{X}^{\mathrm{H}}\right)^{-1}\right)_{i,n}\right) \\ &\quad + j\mathrm{Im}\left(\left(\mathbf{X}^{\mathrm{H}}\right)_{m,i}\left(\left(\mathbf{X}\mathbf{X}^{\mathrm{H}}\right)^{-1}\right)_{i,n}\right)\Bigg] \\ &\quad \times\left(\cos\left(\psi_n(\theta,\phi)\right) + j\sin\left(\psi_n(\theta,\phi)\right)\right)\Bigg\} \\ &\qquad\qquad m = 1, 2, \ldots, M. \end{aligned} \tag{10}$$

Note that, since $\mathbf{a}(\theta,\phi)$ is complex-valued, g_m is also complex-valued.

If we define $\mathbf{g}(\theta,\phi)$ as

$$\mathbf{g}(\theta,\phi) = \left[\; g_1(\theta,\phi) \quad \ldots \quad g_M(\theta,\phi) \;\right], \tag{11}$$

$\mathbf{g}(\theta,\phi)$ is a complex-valued vector function.

Using (11) along with the definition of $g_m(\theta,\phi)$ in (9), it can be easily shown that the cost function of the Capon beamforming algorithm can be written as

$$F(\theta,\phi) = \|\mathbf{g}(\theta,\phi)\|_2^2 = \sum_{m=1}^{M}|g_m(\theta,\phi)|^2. \tag{12}$$

Let $f_{2m-1}(\theta,\phi)$ and $f_{2m}(\theta,\phi)$ in (5) be given by the real part and the imaginary part of $g_m(\theta,\phi)$, respectively. From (10), we have, for $m = 1, 2, \ldots, M$,

$$\begin{aligned} f_{2m-1}(\theta,\phi) &\equiv \mathrm{Re}\left[g_m\left(\theta,\phi\right)\right] \\ &= \sqrt{M}\mathrm{Re}\left(\left(\mathbf{X}^{\mathrm{H}}\right)_{m,i}\left(\left(\mathbf{X}\mathbf{X}^{\mathrm{H}}\right)^{-1}\right)_{i,n}\mathbf{a}\left(\theta,\phi\right)\right) \\ &= \sqrt{M}\sum_{n=1}^{N}\sum_{i=1}^{N}\left(\mathrm{Re}\left(\left(\mathbf{X}^{\mathrm{H}}\right)_{m,i}\left(\left(\mathbf{X}\mathbf{X}^{\mathrm{H}}\right)^{-1}\right)_{i,n}\right)\cos(\psi_n(\theta,\phi)\right) \\ &\quad -\mathrm{Im}\left(\left(\mathbf{X}^{\mathrm{H}}\right)_{m,i}\left(\left(\mathbf{X}\mathbf{X}^{\mathrm{H}}\right)^{-1}\right)_{i,n}\right)\sin\left(\psi_n\left(\theta,\phi\right)\right)\Big) \end{aligned} \quad (13)$$

$$\begin{aligned} f_{2m}(\theta,\phi) &= \mathrm{Im}[g_m(\theta,\phi)] = \sqrt{M}\mathrm{Im}\left(\left(\mathbf{X}^{\mathrm{H}}\right)_{m,i}\left(\left(\mathbf{X}\mathbf{X}^{\mathrm{H}}\right)^{-1}\right)_{i,n}\mathbf{a}\left(\theta,\phi\right)\right) \\ &= \sqrt{M}\sum_{n=1}^{N}\sum_{i=1}^{N}\left(\mathrm{Re}\left(\left(\mathbf{X}^{\mathrm{H}}\right)_{m,i}\left(\left(\mathbf{X}\mathbf{X}^{\mathrm{H}}\right)^{-1}\right)_{i,n}\right)\sin(\psi_n(\theta,\phi)\right) \\ &\quad +\mathrm{Im}\left(\left(\mathbf{X}^{\mathrm{H}}\right)_{m,i}\left(\left(\mathbf{X}\mathbf{X}^{\mathrm{H}}\right)^{-1}\right)_{i,n}\right)\cos\left(\psi_n\left(\theta,\phi\right)\right)\Big) \end{aligned} \quad (14)$$

where, for example, $(\mathbf{X}^{\mathrm{H}})_{m,i}$ denotes the entry of the m-th row and the i-th column of a matrix $\mathbf{X}^{\mathrm{H}}$. Similarly, $((\mathbf{X}\mathbf{X}^{\mathrm{H}})^{-1})_{i,n}$ is the entry of the i-th row and the n-th column of a matrix $(\mathbf{X}\mathbf{X}^{\mathrm{H}})^{-1}$.

From the definition of $f_{2m-1}(\theta,\phi)$ and $f_{2m}(\theta,\phi)$, it is clear that the following is true:

$$|g_m(\theta,\phi)|^2 = \left(f_{2m-1}(\theta,\phi)\right)^2 + \left(f_{2m}(\theta,\phi)\right)^2, \quad m = 1,\ldots,M. \quad (15)$$

From (12) and (15), the cost function can also be written in terms of $f_m(\theta,\phi)$ as follows:

$$F(\theta,\phi) = \sum_{m=1}^{M}|g_m(\theta,\phi)|^2 = \sum_{m=1}^{2M}\left(f_m(\theta,\phi)\right)^2. \quad (16)$$

The Jacobian matrix corresponding to the matrix $\mathbf{f}(\theta,\phi)$ in (5) is defined as

$$\mathbf{J}(\theta,\phi) = \begin{bmatrix} \frac{\partial f_1}{\partial\theta} & \frac{\partial f_1}{\partial\phi} \\ \vdots & \vdots \\ \frac{\partial f_{2M}}{\partial\theta} & \frac{\partial f_{2M}}{\partial\phi} \end{bmatrix}. \quad (17)$$

The explicit expressions of the entries of the matrix $\mathbf{J}(\theta,\phi)$ are,

for $m = 1, \ldots, M$,

$$\frac{\partial f_{2m-1}}{\partial \theta} = \sqrt{M} \sum_{n=1}^{N} \sum_{i=1}^{N} 2\pi \frac{r}{\lambda} \cos\phi \sin\left(\theta - \frac{2\pi(n-1)}{N}\right) \times \left(\mathrm{Re}\left(\left(\mathbf{X}^{\mathrm{H}}\right)_{m,i} \left(\left(\mathbf{X}\mathbf{X}^{\mathrm{H}}\right)^{-1}\right)_{i,n}\right) \sin\left(\psi_n\left(\theta,\phi\right)\right) + \mathrm{Im}\left(\left(\mathbf{X}^{\mathrm{H}}\right)_{m,i} \left(\left(\mathbf{X}\mathbf{X}^{\mathrm{H}}\right)^{-1}\right)_{i,n}\right) \cos\left(\psi_n\left(\theta,\phi\right)\right)\right) \quad (18)$$

$$\frac{\partial f_{2m-1}}{\partial \phi} = \sqrt{M} \sum_{n=1}^{N} \sum_{i=1}^{N} 2\pi \frac{r}{\lambda} \sin\phi \cos\left(\theta - \frac{2\pi(n-1)}{N}\right) \times \left(\mathrm{Re}\left(\left(\mathbf{X}^{\mathrm{H}}\right)_{m,i} \left(\left(\mathbf{X}\mathbf{X}^{\mathrm{H}}\right)^{-1}\right)_{i,n}\right) \sin\left(\psi_n\left(\theta,\phi\right)\right) + \mathrm{Im}\left(\left(\mathbf{X}^{\mathrm{H}}\right)_{m,i} \left(\left(\mathbf{X}\mathbf{X}^{\mathrm{H}}\right)^{-1}\right)_{i,n}\right) \cos\left(\psi_n\left(\theta,\phi\right)\right)\right) \quad (19)$$

$$\frac{\partial f_{2m}}{\partial \theta} = \sqrt{M} \sum_{n=1}^{N} \sum_{i=1}^{N} (-) 2\pi \frac{r}{\lambda} \sin\phi \cos\left(\theta - \frac{2\pi(n-1)}{N}\right) \times \left(\mathrm{Re}\left(\left(\mathbf{X}^{\mathrm{H}}\right)_{m,i} \left(\left(\mathbf{X}\mathbf{X}^{\mathrm{H}}\right)^{-1}\right)_{i,n}\right) \cos\left(\psi_n\left(\theta,\phi\right)\right) - \mathrm{Im}\left(\left(\mathbf{X}^{\mathrm{H}}\right)_{m,i} \left(\left(\mathbf{X}\mathbf{X}^{\mathrm{H}}\right)^{-1}\right)_{i,n}\right) \sin\left(\psi_n\left(\theta,\phi\right)\right)\right) \quad (20)$$

$$\frac{\partial f_{2m}}{\partial \phi} = \sqrt{M} \sum_{n=1}^{N} \sum_{i=1}^{N} (-) 2\pi \frac{r}{\lambda} \sin\phi \cos\left(\theta - \frac{2\pi(n-1)}{N}\right) \times \left(\mathrm{Re}\left(\left(\mathbf{X}^{\mathrm{H}}\right)_{m,i} \left(\left(\mathbf{X}\mathbf{X}^{\mathrm{H}}\right)^{-1}\right)_{i,n}\right) \cos\left(\psi_n\left(\theta,\phi\right)\right) - \mathrm{Im}\left(\left(\mathbf{X}^{\mathrm{H}}\right)_{m,i} \left(\left(\mathbf{X}\mathbf{X}^{\mathrm{H}}\right)^{-1}\right)_{i,n}\right) \sin\left(\psi_n\left(\theta,\phi\right)\right)\right). \quad (21)$$

Finally, the update $[\theta_{\mathrm{LM}}\ \phi_{\mathrm{LM}}]$ in the LM algorithm is obtained from [4, 5]

$$\left[\mathbf{J}^{\mathrm{T}}\mathbf{J} + \mu\mathbf{I}\right] \left[\theta_{\mathrm{LM}}\ \phi_{\mathrm{LM}}\right]^{\mathrm{T}} = -\mathbf{J}^{\mathrm{T}}\mathbf{f}, \quad (22)$$

where $\mathbf{J}$ and $\mathbf{f}$ are defined in (17) and (5), respectively.

In Fig. 1, we outline the LM algorithm where k denotes the number of the iterations [4].

$\mathbf{L}(\theta_{\mathrm{LM}}, \phi_{\mathrm{LM}})$ in Fig. 1 is defined as [4, 5]

$$\mathbf{L}(\theta_{\mathrm{LM}}, \phi_{\mathrm{LM}}) = F(\theta, \phi) + [\ \theta_{\mathrm{LM}} \quad \phi_{\mathrm{LM}}\ ]\,\mathbf{J}(\theta, \phi)^{\mathrm{T}}\,\mathbf{f}(\theta, \phi) + \frac{1}{2}[\theta_{\mathrm{LM}} \quad \phi_{\mathrm{LM}}]\,\mathbf{J}(\theta, \phi)^{\mathrm{T}}\,\mathbf{J}(\theta, \phi)\,[\theta_{\mathrm{LM}} \quad \phi_{\mathrm{LM}}]^{\mathrm{T}}. \quad (23)$$

Due to $\mu > 0$, the coefficient matrix is positive definite, which makes $[\theta_{\mathrm{LM}}\ \phi_{\mathrm{LM}}]^{\mathrm{T}}$ be a descent direction. When μ is very large, we get

$$[\ \theta_{\mathrm{LM}} \quad \phi_{\mathrm{LM}}\ ]^{\mathrm{T}} \simeq -\frac{1}{\mu}\mathbf{J}^{\mathrm{T}}\mathbf{f} \quad (24)$$

which is a short step in the steepest descent direction. Therefore, we choose large μ when the current estimates are assumed to be very far from the solution. This is good if the current iterate is far from the solution. If μ is very small, then the updates of the LM method are approximately equal to the updates of the Newton method, which is a good step in the final stages of the iteration [4].

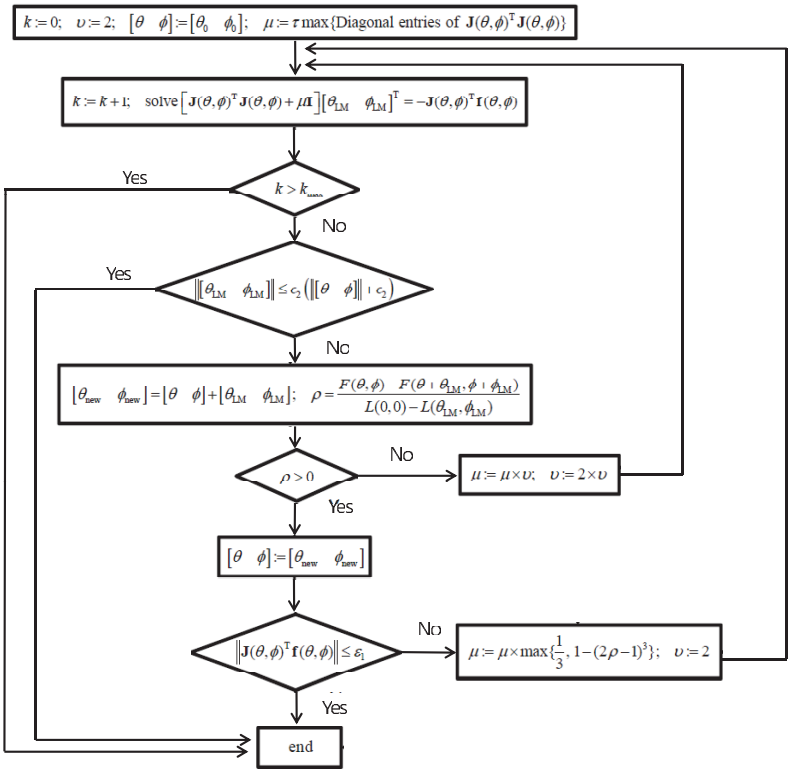

Figure 1. Flow chart of the Levenberg-Marquardt algorithm [4].

τ can be chosen to be a small value of $\tau = 10^{-6}$ if the initial estimate, $[\theta_0, \phi_0]$, is assumed to be close to the solution. Otherwise, τ is chosen to be larger value of $\tau = 10^{-3}$ [4].

The stopping criterion reflects that, at a global minimizer, $\mathbf{J}^{\mathrm{T}}\mathbf{f}$ is given by $\mathbf{J}^{\mathrm{T}}\mathbf{f}\left(\theta^{\mathrm{final}}, \phi^{\mathrm{final}}\right) = \mathbf{0}$. Therefore, practically, the criterion can be

$$\left\|\mathbf{J}(\theta,\, \phi)^{\mathrm{T}}\mathbf{f}(\theta,\, \phi)\right\|_{\infty} \leq \epsilon_1, \tag{25}$$

where ϵ_1 is a small positive number. Another stopping criterion is $\|[\theta_{\mathrm{LM}} \quad \phi_{\mathrm{LM}}]\| \leq \epsilon_2\left([\theta \quad \phi] + \epsilon_2\right)$, which is true when the update in $[\theta, \phi]$ is small.

3. NUMERICAL RESULTS

In this section, the validity of the proposed scheme is illustrated via numerical results. In the numerical results, the UCA with five elements is employed, and the extension to other array structure is straightforward. Therefore, $\mathbf{f}\left(\theta, \phi\right)$ is obtained from (13) and (14), and $\mathbf{J}\left(\theta, \phi\right)$ is given by (18)–(21), where $\psi_n\left(\theta, \phi\right)$ is in (4). The radius of the UCA is equal to 0.679λ.

The parameters used for the results shown in Fig. 2 are specified. Both ϵ_1 and ϵ_2 in Fig. 1 are chosen to be 10^{-5}. The maximum number of the iteration which corresponds to $k_{\max}$ in Fig. 1 is 100.

τ is set to be 1.0. Note that θ_0 and ϕ_0 in Fig. 1 is the estimates obtained from the Capon algorithm with the coarse exhaustive search. Therefore, $\mathbf{J}(\theta = \theta_0, \phi = \phi_0)$ is dependent on the values of θ_0 and ϕ_0, so is the value of μ.

The RMSE (root mean square error) and operation time in Fig. 2 is obtained from $Q = 100$ repetitions. $\theta_1^{(\mathrm{true})}$ and $\phi_1^{(\mathrm{true})}$ denote the true azimuth angle and the true elevation angle of the first incident signal, respectively. Similarly, those of the second incident signal are represented by $\theta_2^{(\mathrm{true})}$ and $\phi_2^{(\mathrm{true})}$, respectively.

The RMSE's of the estimate of the azimuth and that of the elevation are calculated as, for $i = 1, 2$,

$$\mathrm{RMSE}(\theta_i) = \left[\frac{\sum_{q=1}^{Q}\left(\theta_i^{(\mathrm{true})} - \hat{\theta}_i^{(q)}\right)^2}{Q}\right]^{1/2} \tag{26}$$

$$\mathrm{RMSE}(\phi_i) = \left[\frac{\sum_{q=1}^{Q} \left(\phi_i^{(\mathrm{true})} - \hat{\phi}_i^{(q)} \right)^2}{Q} \right]^{1/2} \tag{27}$$

where $\hat{\theta}_i^{(q)}$ and $\hat{\phi}_i^{(q)}$ denote the estimates of the azimuth angle and the elevation angle of the i-th signal corresponding to the q-th trial out of Q repetitions.

The execution time as well as the RMSE is illustrated to quantitatively describe the computational complexity of each scheme. The matlab function 'etime' is used to measure the execution time of each scheme.

In Fig. 2, for two incident signals, we compared the performance of the standard Capon algorithm of coarse exhaustive grid search followed by the LM optimization with that of the standard Capon algorithm of fine exhaustive grid search. The purpose is to illustrate the fact that the proposed scheme still works for more than one incident signal.

$[\Delta\theta^{\mathrm{coarse}}, \Delta\phi^{\mathrm{coarse}}]$ and $[\Delta\theta^{\mathrm{fine}}, \Delta\phi^{\mathrm{fine}}]$ denote the search step of the coarse exhaustive grid search and the fine exhaustive grid search, respectively.

In Fig. 2(a), we set $[\Delta\theta^{\mathrm{fine}}, \Delta\phi^{\mathrm{fine}}] = [2^\circ, 2^\circ]$, and $[\Delta\theta^{\mathrm{coarse}}, \Delta\phi^{\mathrm{coarse}}] = [4^\circ, 4^\circ]$. The corresponding parameters for Fig. 2(b) are given by $[\Delta\theta^{\mathrm{fine}}, \Delta\phi^{\mathrm{fine}}] = [2^\circ, 2^\circ]$, and $[\Delta\theta^{\mathrm{coarse}}, \Delta\phi^{\mathrm{coarse}}] = [7^\circ, 7^\circ]$, and those for Fig. 2(c) are specified as $[\Delta\theta^{\mathrm{fine}}, \Delta\phi^{\mathrm{fine}}] = [4^\circ, 4^\circ]$, and $[\Delta\theta^{\mathrm{coarse}}, \Delta\phi^{\mathrm{coarse}}] = [7^\circ, 7^\circ]$. We arbitrarily choose $\Delta\theta^{\mathrm{coarse}} = \Delta\phi^{\mathrm{coarse}}$ and $\Delta\theta^{\mathrm{fine}} = \Delta\phi^{\mathrm{fine}}$.

In the upper figures of Figs. 2(a)–2(c), the results with legend 'CA Sig.1' and 'CA Sig.2' refer to the RMSE of the first incident signal and that of the second incident signal, respectively, of the standard Capon algorithm implemented with the fine exhaustive search with $[\Delta\theta = \Delta\theta^{\mathrm{fine}}, \Delta\phi = \Delta\phi^{\mathrm{fine}}]$. The results with 'CA+LM Sig.1' and 'CA+LM Sig.2' refer to the RMSE of the first signal and the second signal, respectively, of the Capon algorithm with coarse exhaustive search with $[\Delta\theta = \Delta\theta^{\mathrm{coarse}}, \Delta\phi = \Delta\phi^{\mathrm{coarse}}]$ followed by the LM optimization.

In the lower figures of Figs. 2(a)–2(c), the results with legend strings of 'CA' and 'CA+LM' refer to the time required for the numerical simulation of the standard Capon algorithm with fine exhaustive search with $[\Delta\theta = \Delta\theta^{\mathrm{fine}}, \Delta\phi = \Delta\phi^{\mathrm{fine}}]$ and the Capon algorithm with coarse exhaustive search with $[\Delta\theta = \Delta\theta^{\mathrm{coarse}}, \Delta\phi = \Delta\phi^{\mathrm{coarse}}]$ followed by the LM algorithm, respectively.

In evaluating the performance of the proposed scheme, two criteria

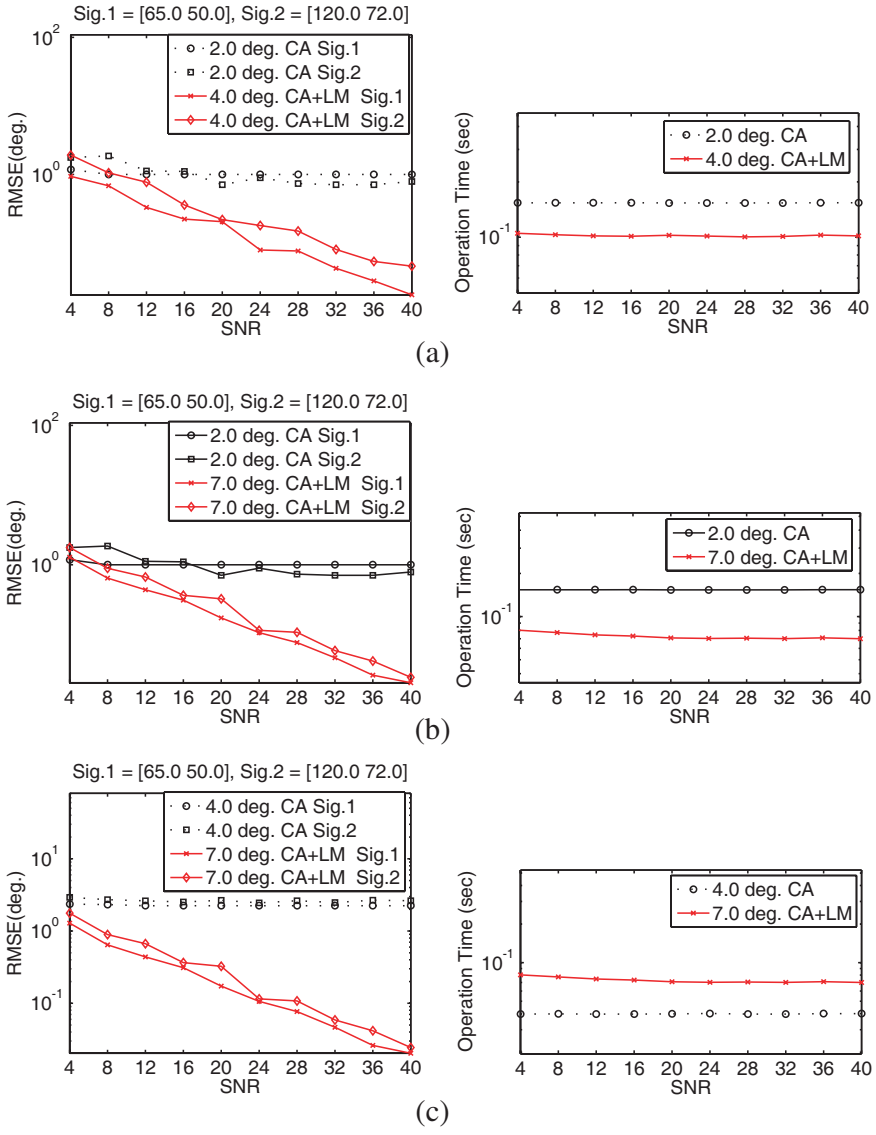

Figure 2. Comparison of the standard Capon algorithm with fine exhaustive grid search with that of the Capon algorithm with coarse exhaustive grid search followed by the LM optimization. (a) $\left[\Delta\theta^{\text{fine}}, \Delta\phi^{\text{fine}}\right] = [2°, 2°]$, $\left[\Delta\theta^{\text{coarse}}, \Delta\phi^{\text{coarse}}\right] = [4°, 4°]$. (b) $\left[\Delta\theta^{\text{fine}}, \Delta\phi^{\text{fine}}\right] = [2°, 2°]$, $\left[\Delta\theta^{\text{coarse}}, \Delta\phi^{\text{coarse}}\right] = [7°, 7°]$. (c) $\left[\Delta\theta^{\text{fine}}, \Delta\phi^{\text{fine}}\right] = [4°, 4°]$, $\left[\Delta\theta^{\text{coarse}}, \Delta\phi^{\text{coarse}}\right] = [7°, 7°]$

of the RMSE and the operation time are used. RMSE is used as a measure of the estimation accuracy, and the operation time is a measure of the computational burden. We compare the RMSE and the operation time of the proposed scheme with those of the standard Capon algorithm to illustrate how much improvement our proposed scheme shows over the standard Capon algorithm.

In the upper figures of Fig. 2, we confirm that the RMSE's of the proposed scheme are smaller than those of the standard implementation of the Capon algorithm, which confirms that the proposed scheme is better than the standard Capon algorithm in terms of the estimation accuracy. Note that the RMSE's of the proposed scheme are much smaller than those of the standard Capon algorithm for high SNR.

What we illustrate in the lower figures of Fig. 2 is that the proposed scheme is better than the standard Capon algorithm in terms of the computational burden as well as the RMSE. In the lower figures of Fig. 2, we confirm that the execution times of the proposed scheme are smaller than those of the standard Capon algorithm, which illustrates that the proposed scheme is superior to the standard Capon algorithm in terms of the computational burden.

Note that y-axis of all the figures in Fig. 2 is in log-scale, not in linear scale to more clearly quantify the RMSE and the execution time. We can see in Fig. 2 that the LM implementation of the Capon algorithm is superior to the standard Capon algorithm for all three cases in terms of the RMSE and the computational complexity.

4. CONCLUSION

In this paper, we propose to apply the LM formulation to the optimization of the cost function of the Capon beamforming algorithm. We have compared the performance of the LM implementation of the Capon algorithm with that of the standard Capon algorithm in terms of the estimation accuracy and the computational complexity.

We consider the array structure of the UCA to be able to uniquely estimate the azimuth and elevation simultaneously, but it is quite straightforward to extend the proposed scheme to an arbitrary array structure by simply modifying the array vector consistently with the specific array structure as long as the adopted array structure is able to uniquely estimate both the azimuth angle and the elevation angle. In addition, the proposed scheme can also be applied to the other AOA estimation algorithm by simply modifying the cost function consistently with the adopted AOA estimation algorithm. In numerical results, we demonstrate the validity of the proposed scheme in terms of the estimation accuracy and the computational complexity.

ACKNOWLEDGMENT

This research was supported by Basic Science Research Program through the National Research Foundation of Korea (NRF) funded by the Ministry of Education, Science and Technology (2012-0002347).

REFERENCES

1. Capon, J., "High resolution frequency-wavenumber spectrum analysis," *Proceedings of the IEEE*, Vol. 57, 1408–1418, 1969.
2. Tweg, R. and B. Porat, "Numerical optimization method for array signal processing," *IEEE Trans. Aerospace and Electronic Systems*, Vol. 35, 549–565, 1999.
3. Selva, J., "An efficient Newton-type method for the computation of ML estimators in a uniform linear array," *IEEE Trans. Signal Processing*, Vol. 53, No. 6, 2036–2045, 2005.
4. Madsen, K, H. B. Nielsen, and O. Tingleff, *Methods for Non-linear Least Squares Problem*, 2nd Edition, Technical University of Denmark, 2004.
5. More, J., "The Levenberg-Marquardt algorithm: Implementation and theory," *Lecture Notes in Mathematics*, Vol. 630, 105–116, 1798.
6. Lee, J.-H, S.-W. Cho, and H.-S. Kim, "Newton-type method in spectrum estimation-based AOA estimation," *Electronics Express*, Vol. 9, No. 12, 1036–1043, 2012.
7. Lee J.-H., S.-W. Cho, and I.-S. Choi, "Simple expressions of CEP and covariance matrix for localization using LOB measurements for circular trajectory," *Electronics Express*, Vol. 9, No. 14, 1221–1229, 2012.
8. Liang, J. and D. Liu, "Two L-shaped array-based 2-D DOAs estimation in the presence of mutual coupling," *Progress In Electromagnetics Research*, Vol. 112, 273–298, 2011.
9. Cheng, S.-C. and K.-C. Lee, "Reducing the array size for DOA estimation by an antenna mode switch technique," *Progress In Electromagnetics Research*, Vol. 131, 117–134, 2012.
10. Solimene R., A. Dell'Aversano, and G. Leone, "Interferometric time reversal MUSIC for small scatterer localization," *Progress In Electromagnetics Research*, Vol. 131, 243–258, 2012.
11. Lee, J.-H., Y.-S. Jeong, S.-W. Cho, W.-Y. Yeo, and K. S. J. Pister, "Application of the newton method to improve the accuracy of TOA estimation with the beamforming algorithm and the MUSIC

algorithm," *Progress In Electromagnetics Research*, Vol. 116, 475–515, 2011.

12. Chen, Y. L. and J.-H. Lee, "Finite data performance analysis of LCMV antenna array beamformers with and without signal blocking," *Progress In Electromagnetics Research*, Vol. 130, 281–317, 2012.
13. Hong, T., M.-Z. Song, and Y. Liu, "RF directional modulation technique using a switched antenna array for communication and direction-finding Applications," *Progress In Electromagnetics Research*, Vol. 120, 195–213, 2011.
14. Bencheikh, M. L. and Y. Wang, "Combined ESPRIT-RootMUSIC for DOA-DOD estimation in polarimetric bistatic MIMO radar," *Progress In Electromagnetics Research Letters*, Vol. 22, 109–117, 2011.
15. Peng, H., Z. Yang, and T. Yang, "Calibration of a six-port receiver for direction finding using the artificial neural network technique," *Progress In Electromagnetics Research Letters*, Vol. 27, 17–24, 2011.
16. Kim, Y. and H. Ling, "Direction of arrival estimation of humans with a small sensor array using an artificial neural network," *Progress In Electromagnetics Research B*, Vol. 27, 127–149, 2011.
17. Elshennawy, W. S., A. M. Attiya, E. A. H. Hashish, and I. A. Eshrah, "Direction of arrival estimation for nonuniform planar array based on piecewise interpolation method," *Progress In Electromagnetics Research B*, Vol. 38, 241–259, 2012.
18. Zhou, Q.-C., H. Gao, F. Wang, and J. Shi, "Modified DOA estimation methods with unknown source number based on projection pretransformation," *Progress In Electromagnetics Research B*, Vol. 38, 387–403, 2012.
19. Zaharis, Z. D., C. Skeberis, and T. D. Xenos, "Improved antenna array adaptive beamforming with low side lobe level using a novel adaptive invasive weed optimization method," *Progress In Electromagnetics Research*, Vol. 124, 137–150, 2012.
20. Li, W.-X., Y.-P. Li, and W.-H. Yu, "On adaptive beamforming for coherent interference suppression via virtual antenna array," *Progress In Electromagnetics Research*, Vol. 125, 165–184, 2012.
21. Zaharis, Z. D., K. A. Gotsis, and J. N. Sahalos, "Comparative study of neural network training applied to adaptive beamforming of antenna arrays," *Progress In Electromagnetics Research*, Vol. 126, 269–283, 2012.
22. Liu, X., T. Jiang, L. Yang, and H.-B. Zhu, "Constrained trilinear

decomposition with application to array signal processing," *Progress In Electromagnetics Research*, Vol. 128, 195–214, 2012.

23. Mallipeddi, R., J. P. Lie, P. N. Suganthan, S. G. Razul, and C. M. S. See, "A differential evolution approach for robust adaptive beamforming based on joint estimation of look direction and Array Geometry," *Progress In Electromagnetics Research*, Vol. 119, 381–394, 2011.
24. Eom, S. Y., Y.-B. Jung, S. A. Ganin, and A. V. Shishlov, "A cylindrical shaped-reflector antenna with a linear feed array for shaping complex beam patterns," *Progress In Electromagnetics Research*, Vol. 119, 477–495, 2011.
25. Zaharis, Z. D. and T. V. Yioultsis, "A novel adaptive beamforming technique applied on linear antenna arrays using adaptive mutated boolean PSO," *Progress In Electromagnetics Research*, Vol. 117, 165–179, 2011.
26. Li, W.-T., Y.-Q. Hei, and X.-W. Shi, "Pattern synthesis of conformal arrays by a modified particle swarm optimization," *Progress In Electromagnetics Research*, Vol. 117, 237–252, 2011.
27. Wang, W.-B., Q. Feng, and D. Liu, "Application of chaotic particle swarm optimization algorithm to pattern synthesis of antenna arrays," *Progress In Electromagnetics Research*, Vol. 115, 173–189, 2011.
28. Li, R., L. Xu, X.-W. Shi, N. Zhang, and Z.-Q. Lv, "Improved differential evolution strategy for antenna array pattern synthesis problems," *Progress In Electromagnetics Research*, Vol. 113, 429–441, 2011.
29. Zaharis, Z. D., K. A. Gotsis, and J. N. Sahalos, "Adaptive beamforming with low side lobe level using neural networks trained by mutated boolean PSO," *Progress In Electromagnetics Research*, Vol. 127, 139–154, 2012.
30. Zaharis, Z. D., "A modified Taguchi's optimization algorithm for beamforming applications," *Progress In Electromagnetics Research*, Vol. 127, 553–569, 2012.
31. Wu, X. P., J.-M. Shi, Z. S. Chen, and B. Xu, "A new plasma antenna of beam-forming," *Progress In Electromagnetics Research*, Vol. 126, 539–553, 2012.
32. Jeong, S.-H., H.-Y. Yu, J.-E. Lee, J.-N. Oh, and K.-H. Lee, "A multi-beam and multi-range radar with FMCW and digital beam forming for automotive applications," *Progress In Electromagnetics Research*, Vol. 124, 285–299, 2012.
33. Lu, S., J. Sun, G. Wang, and Y.-L. Lu, "A mixing vector based

an affine combination of two adaptive filters for sensor array beamforming," *Progress In Electromagnetics Research*, Vol. 122, 361–387, 2012.

34. Mallipeddi, R., J. P. Lie, S. G. Razul, P. N. Suganthan, and C. M. S. See, "Robust adaptive beamforming based on covariance matrix reconstruction for Look direction mismatch," *Progress In Electromagnetics Research Letters*, Vol. 25, 37–46, 2011.
35. Lee, J.-H., G.-W. Jung, and W.-C. Tsai, "Antenna array beamforming in the presence of spatial information uncertainties," *Progress In Electromagnetics Research B*, Vol. 31, 139–156, 2011.
36. Lee, J.-H., "Robust antenna array beamforming under cycle frequency mismatch," *Progress In Electromagnetics Research B*, Vol. 35, 307–328, 2011.
37. Jabbar, A. N., "A novel ultra-fast ultra-simple adaptive blind beamforming algorithm for smart antenna arrays," *Progress In Electromagnetics Research B*, Vol. 35, 329–348, 2011.
38. Huang, C.-C. and J.-H. Lee, "Robust adaptive beamforming using a fully data-dependent loading technique," *Progress In Electromagnetics Research B*, Vol. 37, 307–325, 2012.
39. Cho, S.-W. and J.-H. Lee, "Effect of threshold value on the performance of natural frequency-based radar target recognition," *Progress In Electromagnetics Research*, Vol. 135, 527–562, 2013.
40. Lee, J.-H., S.-W. Cho, S.-H. Park, and K.-T. Kim, "Performance analysis of radar target recognition using natural frequency: Frequency domain approach," *Progress In Electromagnetics Research*, Vol. 132, 315–345, 2012.
41. Lee, J.-H. and S.-H. Jeong, "Performance of natural frequency-based target detection in frequency domain," *Journal of Electromagnetic Waves and Applications*, Vol. 26, Nos. 17–18, 2426–2437, 2012.
42. Lee, J.-H. and H.-T. Kim, "Comments on extraction of the natural frequencies of a radar target from a measured response using E-pulse techniques," *IEEE Transactions Antennas and Propagation*, Vol. 53, No. 11, 3853–3855, Nov. 2005.
43. Lee, J.-H. and H.-T. Kim, "Radar target recognition based on late time representation: Closed form expression for criterion," *IEEE Transactions on Antennas and Propagation*, Vol. 54, No. 9, 2455–2462, 2006.
44. Li, J. and P. Stoica, *Robust Adaptive Beamforming*, Wiley-Interscience, 2006.
45. Li, J., P. Stoica, and Z. Wang, "On robust Capon beamforming

and diagonal loading," *IEEE Transactions on Signal Processing*, Vol. 51, No. 7, 1702–1715, 2003.

46. Li, J., P. Stoica, and Z. Wang, "Doubly constrained robust Capon beamformer," *IEEE Transactions on Signal Processing*, Vol. 52, 2407–2423, 2004.
47. Du, Lin, J. Li, and P. Stoica, "Fully automatic computation of diagonal loading levels for robust adaptive beamforming," *IEEE Transactions on Aerospace and Electronics Systems*, Vol. 46, 449–458, 2010.
48. Elnashar, A., S. Elnoubi, and H. El-Mikati, "Further study on robust adaptive beamforming with optimum diagonal loading," *IEEE Transactions on Antennas and Propagation*, Vol. 54, 3647–3658, 2006.